

# Effect of Matrix Composition on the Aging of CFRC

Amnon Katz & Arnon Bentur

National Building Research Institute, Department of Civil Engineering, Technion — Israel Institute of Technology, Haifa 32000, Israel

(Received 21 May 1994; accepted 4 August 1994)

## Abstract

*Properties of polyacrylonitrile (PAN) type carbon fiber reinforced cementitious composites were tested after aging in water at 20 and 60°C for up to 10 and 7 months, respectively. Composites with water–binder ratios of 0.25 and 0.40 and silica-fume contents of 0–28% were investigated. The results show an increase in flexural strength and toughness with time up to a maximum at two–four weeks, and a reduction thereafter, with a loss of up to 65% of the maximum value. The loss was higher at 60°C aging temperature and at higher silica-fume contents. Flexural strength and microhardness tests of the matrix showed a continuous increase with time, in agreement with observations of densification of the matrix and refinement of the pore structure, as observed by mercury intrusion porosimetry (MIP) tests.*

*Maximum flexural strength and toughness values at early ages were obtained with mixes containing 7–14% of silica-fume. Higher silica-fume contents led to reduction in the early age strength and toughness values, although the matrix became denser and exhibited finer pore structure.*

*SEM observations of the fractured specimens after loading showed crumbling of the matrix near inclined fibers, suggesting that fiber bending rupture is a major mechanism responsible for loss in mechanical properties which accompanied the densening of the matrix with increase in silica-fume content and age.*

## 1 INTRODUCTION

The use of carbon fiber reinforced cement and concrete is drawing considerable interest. The excellent mechanical properties of the carbon fiber combined with its resistivity to the alkaline environment of the cement suggest that carbon

fiber has the potential for becoming an effective reinforcement for cementitious materials. Most of the work in this area has dealt with the short term properties, mainly the mechanical performances<sup>1–3</sup> and workability of the fresh mix.<sup>3–5</sup>

According to Bentur and Mindess<sup>6</sup> and Laws<sup>7</sup> there may be cases when the reinforcement of Portland cement with fibers of high aspect ratio and bond strength, may result in loss in toughness when the bond strength exceeds a critical value, as may happen with time. This phenomenon is more likely to occur when using fine carbon fibers dispersed in high strength cement matrix. However, only few works have dealt with the study of the long term properties of carbon fiber reinforced cements (CFRC).

Akihama *et al.*<sup>1</sup> tested the long term properties of Pitch type carbon fiber reinforcing lightweight concrete. They found an unexplained reduction of approximately 10% in the flexural strength after reaching a maximum at four weeks, for specimens cured in hot water (75°C) for five months. A similar trend was also observed by Ali *et al.*<sup>8</sup> for PAN type carbon fibers cured in 50°C for one year. However, as the reduction was small, it was suggested that CFRC properties do not change with time.<sup>9</sup>

The object of the present work was to resolve to some extent certain formulations of CFRC that may show signs of loss of mathematical properties during aging, in particular compositions with a dense matrix. The work carried out here was based on the use of PAN type carbon fibers. The present paper presents results of mechanical properties and microstructure.

## 2 EXPERIMENTAL PROCEDURE

The cement used was ASTM type I Portland cement. Silica-fume (SF) was of 92.7% SiO<sub>2</sub> with

a specific surface area of  $18\,300\text{ m}^2\text{ kg}^{-1}$  and a density of  $2110\text{ kg m}^{-3}$ . The carbon fibers were of the PAN type, and some of their properties are described in Table 1.

Ten mixes of paste were prepared at two different water–binder (w/b) ratios (0.25 and 0.40) and five different silica-fume contents (0, 7, 14, 21 and 28% by weight of the binder). Two types of specimen were prepared for the above matrix compositions: (a) pastes reinforced with 6% by volume of fibers; and (b) unreinforced pastes. All materials were mixed in a sigma ( $\Sigma$ ) type mixer, which consisted of two horizontal blades with the shape of  $\Sigma$ , providing very high mixing power, as needed for this kind of dense and high viscosity material, which enables the introduction of a relatively high volume of fibers.

The paste was prepared by adding the cement and silica-fume to the water and mixing together for 5 min. For the reinforced pastes, fibers were gradually added to the paste within 1 min and mixing was carried out for an additional 15 min until a homogeneous material was achieved.

The workability of the fresh mix was tested on a flow table and the results were presented elsewhere.<sup>10</sup>

Thin slab specimens with size  $140\times120\times10\text{ mm}$  were cast and kept sealed for a day or two. After demolding, all specimens were kept in water at  $20^\circ\text{C}$ . After three days some of the specimens were placed in a hot water bath at  $60^\circ\text{C}$  for the purpose of accelerated aging. This method of aging enables the basic structure of the cement matrix, which is developed mainly at an early age, to be developed under normal conditions. The high temperature affects mostly the aging process without damaging the early age structure.<sup>11</sup> A temperature of  $60^\circ\text{C}$  is recommended by the international standard (ISO/DIS 8366-Fiber Cement Flat Sheet, 1991) for testing FRCs. In the following, the letter H preceding the age refers to aging in hot water, for example: H230 means aging at  $60^\circ\text{C}$  for 230 days. The tests were carried out after 1, 3, 5, 10, 15, 28 and 300 days at  $20^\circ\text{C}$  and after 14, 28, 56, 84 and 230 days at  $60^\circ\text{C}$ .

Table 1. Carbon fiber properties

Type	Tensile strength (MPa)	Modulus of elasticity (GPa)	Ultimate strain (%)	Carbon content (%)	Diameter ( $\mu\text{m}$ )	Length (mm)
PAN	2900	230	1.4	95	6.8	6

On the day of testing, the slab specimen was cut into six small beams of  $20\times120\times10\text{ mm}$ . The three point bending test was performed by an Instron testing machine. The span of the beam was 90 mm and the rate of the crosshead movement was  $0.5\text{ mm min}^{-1}$ . Flexural strength calculated from the maximum load, limit of proportionality (LOP) and toughness were determined for each specimen. Figure 1 represents a typical load–deflection curve on which the points determining the LOP and flexural strength, and the toughness (area under the curve) are marked.

The toughness in this study was defined as the area under the load–deflection curve up to a deflection of 0.8 mm ( $l/110$ ). Other methods of toughness characterization are based on the definition of toughness indexes, such as those proposed by Barr *et al.*<sup>12</sup> and Johnston,<sup>13</sup> which were adopted by ASTM C1018 as a standard testing method. However, the value of the toughness index calculated from these methods is very sensitive to the determination of the load and deflection at first crack. The definition chosen in this work is a more direct representation of the fracture energy associated with fiber pullout.

Plain cement paste specimens without fibers were prepared and tested for bending using the same procedures and aging treatment as the fiber reinforced specimens.

Several tests for evaluating the microstructure were carried out on fragments of the specimens after the flexural test:

- Scanning electron microscope (SEM) observation of the fractured surface to obtain information on the matrix structure around the fiber, as well as on the bulk matrix and the fiber surface.
- Mercury intrusion porosimetry (MIP) to characterize the total porosity and pore size distribution of the composite. Two parameters were calculated from the MIP tests: (a) pore size distribution and (b) the porosity of all pores larger than 3 nm, which were considered to have a strong effect on the mechanical properties of the material.<sup>14</sup> The term ‘total porosity’ in this work will refer to the porosity of all the pores larger than 3 nm, as measured by the MIP.
- Vickers microhardness was determined on some of the specimens in order to evaluate the micro-mechanical properties of the composites. Due to technical difficulties in the preparation of the specimens for the

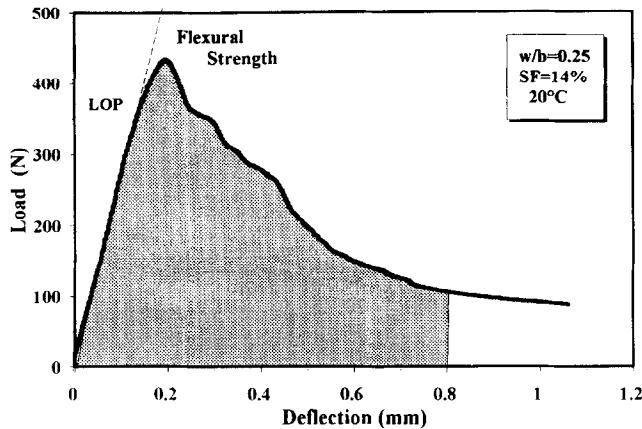


Fig. 1. Typical load-deflection curve.

microhardness tests, only specimens at the age of 300 or H230 days were tested accurately for all the silica-fume contents, while for other ages the results are of qualitative nature only. It should be noted that this method does not allow to evaluate the matrix hardness close to the fiber as the sensitivity of the testing apparatus was  $10\text{ }\mu\text{m}$  and the fiber diameter was  $7\text{ }\mu\text{m}$ . For testing of the hardness close to the fiber, a resolution of approximately  $1\text{ }\mu\text{m}$  is needed, which can not be achieved with the current equipment. Thus, the results here represent the properties of the bulk matrix of the composite.

### 3 RESULTS AND DISCUSSION

#### 3.1 Effect of aging conditions on the mechanical properties of the composite

##### 3.1.1 Flexural strength and toughness

Typical results of age on the flexural strength and toughness are presented in Figs 2(a) and 2(b), respectively, for a composite with a  $w/b$  of 0.25 and silica-fume content of 7%. Figure 3(a) and 3(b) represent the same but for composites with  $w/b$  of 0.40. The dotted lines represent specimens aged at  $60^\circ\text{C}$  and the solid lines represent the specimens aged at  $20^\circ\text{C}$ .

The trends in Figs 2 and 3 are typical of all the specimens. It seemed that at an early age of two–four weeks, the composite gained maximum flexural strength and toughness. After achieving this maximum, a significant reduction in both properties was observed. The magnitude of the reduction was dependent on aging temperature and silica-fume content. For the higher aging

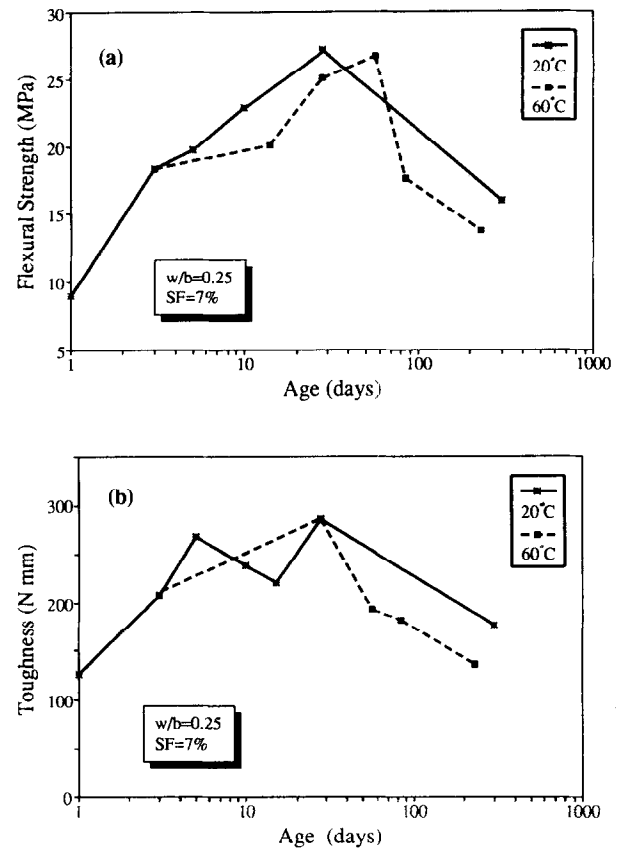


Fig. 2. Development of (a) flexural strength and (b) toughness of composites with  $w/b = 0.25$  and  $SF = 7\%$ .

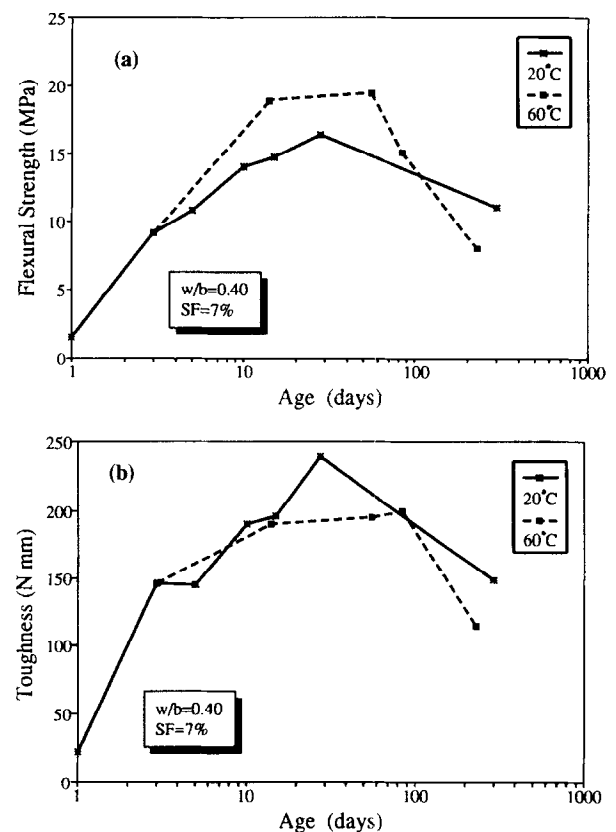


Fig. 3. Development of (a) flexural strength and (b) toughness of composites with  $w/b = 0.40$  and  $SF = 7\%$ .

temperature the values of the maximum strength and toughness achieved at two–four weeks were higher than for the lower aging temperature. However, the reduction afterwards was much greater at the higher temperature, leading to lower values of final flexural strength and toughness than for composites aged at the lower temperature.

Trends of reduction in properties with time were also reported by Akihama *et al.*<sup>1</sup> for low modulus carbon fibers (Pitch type) and weaker matrix. Ali *et al.*<sup>8</sup> reported such trends for continuous high modulus fibers. It is possible that this trend depends on both fiber and matrix properties and, therefore, it is not always clearly observed for every combination of fiber and matrix.

The age effect could be expressed more clearly by presenting the relative residual flexural strength and the relative residual toughness. The relative values are the ratio between the residual flexural strength or toughness at the end of the aging period relative to the maximum achieved at the age of two–four weeks. These values are presented in Figs 4(a) and 4(b) for specimens aged in water at 60°C. For the composites aged in water at 20°C the reduction in the properties was quite similar (approximately 30%), independent of the silica-fume content. It is possible that the higher aging temperature improves the reactivity of the silica-fume to a greater degree than the lower temperature,<sup>15,16</sup> thus, leading to stronger changes in a shorter time.

It can be seen from Fig. 4 that a significant reduction occurred for both flexural strength and toughness. The loss of flexural strength or toughness is more pronounced at the higher silica-fume contents. Specimens of 0% silica-fume lost approximately 35 and 45% of their properties for  $w/b$  of 0.25 and 0.40, respectively. For higher silica-fume contents the loss of properties was 50 and 65%, respectively, and the composite lost most of the flexural strength gained by the addition of the fibers. It will be shown later that after the long aging period the composite flexural strength dropped to values similar to those of the plain matrix. The toughness of the plain matrix was very low, and can be considered as zero. Therefore, even a loss of 75% in the toughness after a long aging period still leaves the composite with some toughness that is significantly higher than the toughness of the plain matrix.

It is possible that loss in properties is associated with additional densening obtained due to the continuation of hydration and pozzolanic reac-

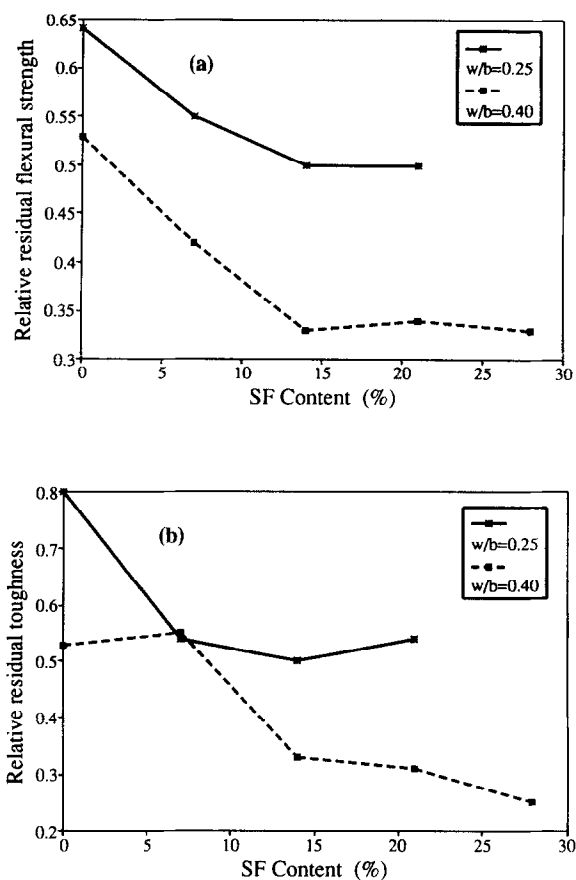


Fig. 4. Effect of silica-fume content on the relative residual flexural strength (a) and toughness (b) of composites aged at 60°C.

tions. Thus, the trends of loss in properties are much more marked in composites of high silica-fume content and higher aging temperature.

### 3.1.2 First crack strength

Trends in the results of first crack strength (limit of proportionality—LOP) were very similar to the results of the flexural strength, i.e.: (a) age effect showing increase in first crack strength at an early age (two–four weeks) and a reduction thereafter; and (b) effect of silica-fume content showing a maximum in first crack strength at silica-fume contents of 7–14%. The typical age effect on the flexural strength and LOP can be seen in the insert in Fig. 5 for a composite of  $w/b = 0.40$  and silica-fume content of 21%, aged at 60°C.

It seems that the increase in flexural strength over the first crack strength is affected by age. At early age and 20°C aging temperature the ratio of LOP/flexural strength was between 0.6 and 0.7, while for later ages it increased to approximately 0.8, as may be seen in Fig. 5. For composites aged

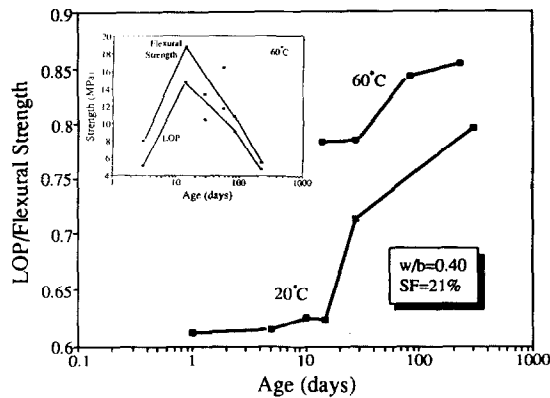


Fig. 5. Effect of age on the ratio LOP/flexural strength. The insert: development with time of LOP and flexural strength for the same mix.

at 60°C this ratio varied from 0.75 at early age up to 0.85 at a later age, as presented in Fig. 5. The increase with age in the LOP/flexural strength ratio indicates a reduced post-crack load bearing capacity, which might be interpreted as reduced toughness in the ascending part of the load-deflection curve, i.e. an increase in brittleness.

### 3.1.3 Effect of silica-fume content on the aging of the composite

The effect of the silica-fume content on the flexural strength and toughness is presented in Fig. 6 for composites of  $w/b = 0.40$ . The trends were similar for the lower  $w/b$  ratio of 0.25.

Two sets of lines are plotted: one for the maximum flexural strength and toughness achieved at ages of two–four weeks, and the other for the flexural strength and toughness at the end of the aging period (300 and H230 days).

The difference between the maximum line and the corresponding line at 300 days or H230 days represents the loss in properties due to aging, both in 20°C and 50°C water. All the lines exhibit a similar trend for a tendency to a maximum at a silica-fume content in the range of 7–14%. A similar effect of silica-fume was reported by Soroushian and Bayasi<sup>17</sup> for steel fiber reinforced concrete.

## 3.2 Properties of the matrix

### 3.2.1 Flexural strength

Test results for the plain matrix can serve as an estimate to the matrix properties in the composite. Typical age effects on the matrix flexural strength is presented in Fig. 7, for pastes aged at 20°C and different silica-fume contents. It is clear from

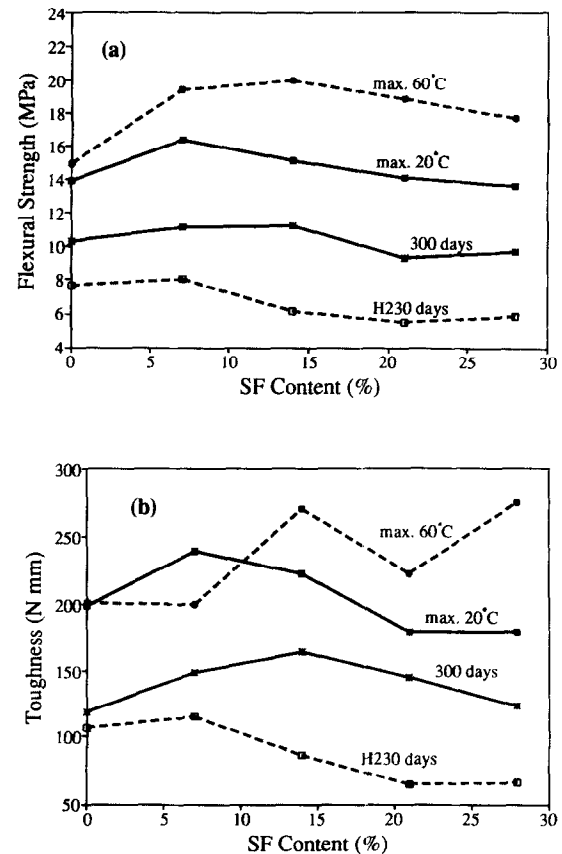


Fig. 6. Effect of silica fume on the (a) flexural strength and (b) toughness of composites of  $w/b = 0.40$  at different ages.

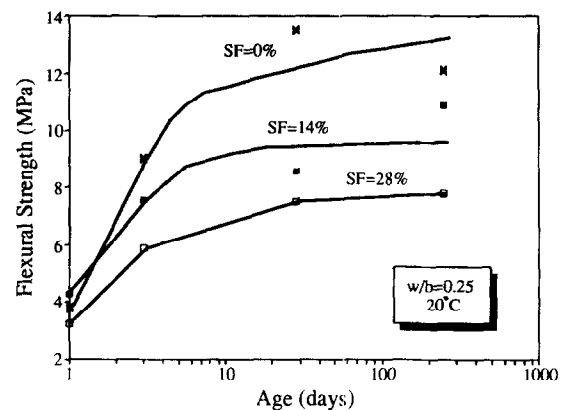


Fig. 7. Development of flexural strength of unreinforced paste of  $w/b = 0.25$ .

Fig. 7 that matrix flexural strength increases gradually with time, and no reduction in strength was seen, contrary to the observations in the composite. Therefore, deterioration of the matrix can not be the cause for the reduction in the composite properties with age.

Evaluation of the effect of silica-fume indicates a reduction in the flexural strength as the silica-

fume content increases, as can be seen in Fig. 8 for paste of  $w/b = 0.40$  at two ages: three days and 28 days (all specimens at the age of 300 days and  $w/b = 0.40$  accidentally broke down during the preparations for testing and could not be tested). This effect is surprising as one could expect higher strength silica-fume pastes due to the refinement in the pore structure. However, an increase in the silica-fume content might be associated also with an increase in micro-cracking due to autogenous shrinkage,<sup>18-20</sup> which affects mainly tensile and flexural strength.

### 3.2.2 Microhardness

Tests were performed under the limitations described earlier, i.e. the results presented the properties of the matrix between the fibers. Test results of specimens of 0 and 28% silica-fume content indicate a gradual increase of the microhardness with age, similar to the increase in the flexural strength of the matrix. This supports the assumption that the matrix properties have not decreased with age and the reduction in the composite properties during aging can not be related to matrix deterioration.

The effect of silica-fume content on the microhardness values at ages of 300 and H230 days (aged at 20°C and 60°C, respectively) is presented in Fig. 9 for the two water-binder ratios. It can be seen that the microhardness decreased as the silica-fume content increased to 14–21%; thereafter, a trend can be observed for a slight increase in the microhardness with increase in the silica-fume content.

This trend is similar to that observed for the flexural strength of the matrix, which tended to

decrease with increasing silica-fume content (Fig. 8). As discussed in the case of flexural strength, this trend is not in agreement with the expected influence of silica-fume content on the pore structure, which densifies with increasing silica-fume content. These results suggest that mechanisms other than pore structure may affect the strength of the matrix, one of the possibilities being autogenous shrinkage which may lead to microcracking and internal damage to the matrix. Paillere *et al.*<sup>21</sup> and Bloom and Bentur<sup>22</sup> considered such an effect.

## 3.3 Microstructure

### 3.3.1 SEM observations

SEM photomicrographs of the fractured surface of the densest composite ( $w/b = 0.25$  and  $SF = 28\%$ ) and the less dense composite ( $w/b = 0.40$  and  $SF = 0\%$ ) are presented in Figs 10 and 11, respectively. It can be seen that in all cases, the matrix structure is uniform throughout, i.e. very close to the fiber, as well as far away from it (Figs 10(a) and 11(b)). Even at higher magnifications (Fig. 12) no transition zone was seen, contrary to typical observations in cementitious composites reinforced with relatively large fibers such as steel<sup>23</sup> or aggregates.<sup>24,25</sup> It might be suggested that the formation of the transition zone depends on the size of the filler; when using small diameter fibers as in this work ( $6.8 \mu\text{m}$ ), which are smaller than most of the cement grains, the transition zone does not develop.

It can also be seen in Fig. 10(a) that the fiber distribution is relatively uniform. Fibers are randomly distributed in the matrix, and each individual filament is well surrounded by the matrix. Uniform distribution and dense matrix

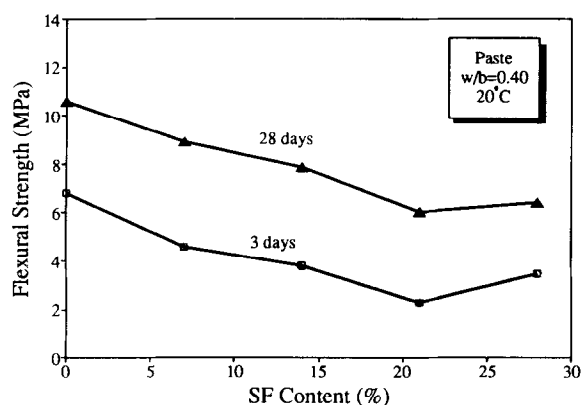


Fig. 8. Effect of silica-fume on the flexural strength of unreinforced paste of  $w/b = 0.40$  at the ages of 3 and 28 days.

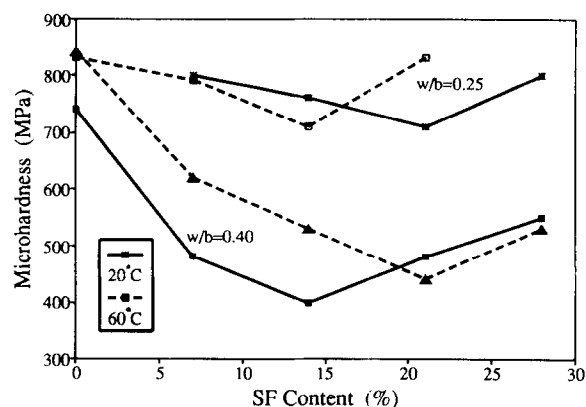
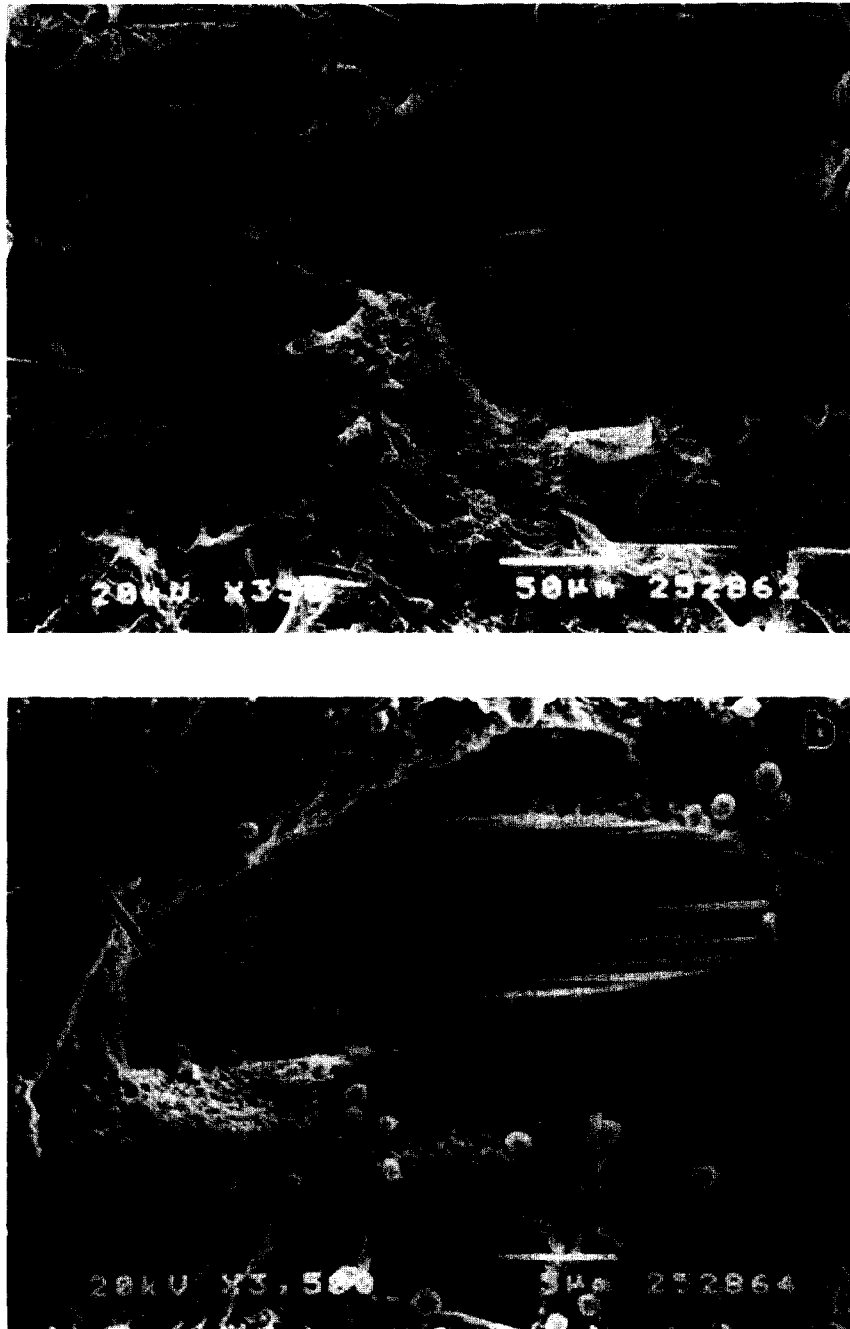


Fig. 9. Effect of silica-fume content on the microhardness of the composite at the ages of 300 and H230 days (aged at 20 and 60°C, respectively).



**Fig. 10.** SEM photomicrograph of a composite of  $w/b = 0.25$  and  $SF = 28\%$  aged in hot water for 56 days. (a) General look, (b) higher magnification at the matrix close to the fiber hole.

around the fiber are basic requirements for adequate performance of a composite material.

When an inclined fiber is pulled out, local compressive stresses are developed in the matrix, leading to crumbling and spalling of the matrix at the point at which the fiber exits the matrix. The arrow in Fig. 11(b) points towards a crumbled zone of this nature. The specimens were cleaned in an ultrasonic bath as part of the preparations

for SEM observation, thus, crumbs were not seen all the time. However, a cavity of the missing crumbled zone can be seen clearly in Figs 10(b) and 11(a), marked by arrows.

Figure 12 presents a high magnification of the fiber surface ( $\times 5000$ ). Such observations were carried out to determine possible signs of damage to the carbon fiber that may occur due to the long exposure (56 days in hot water) in the high alkali-

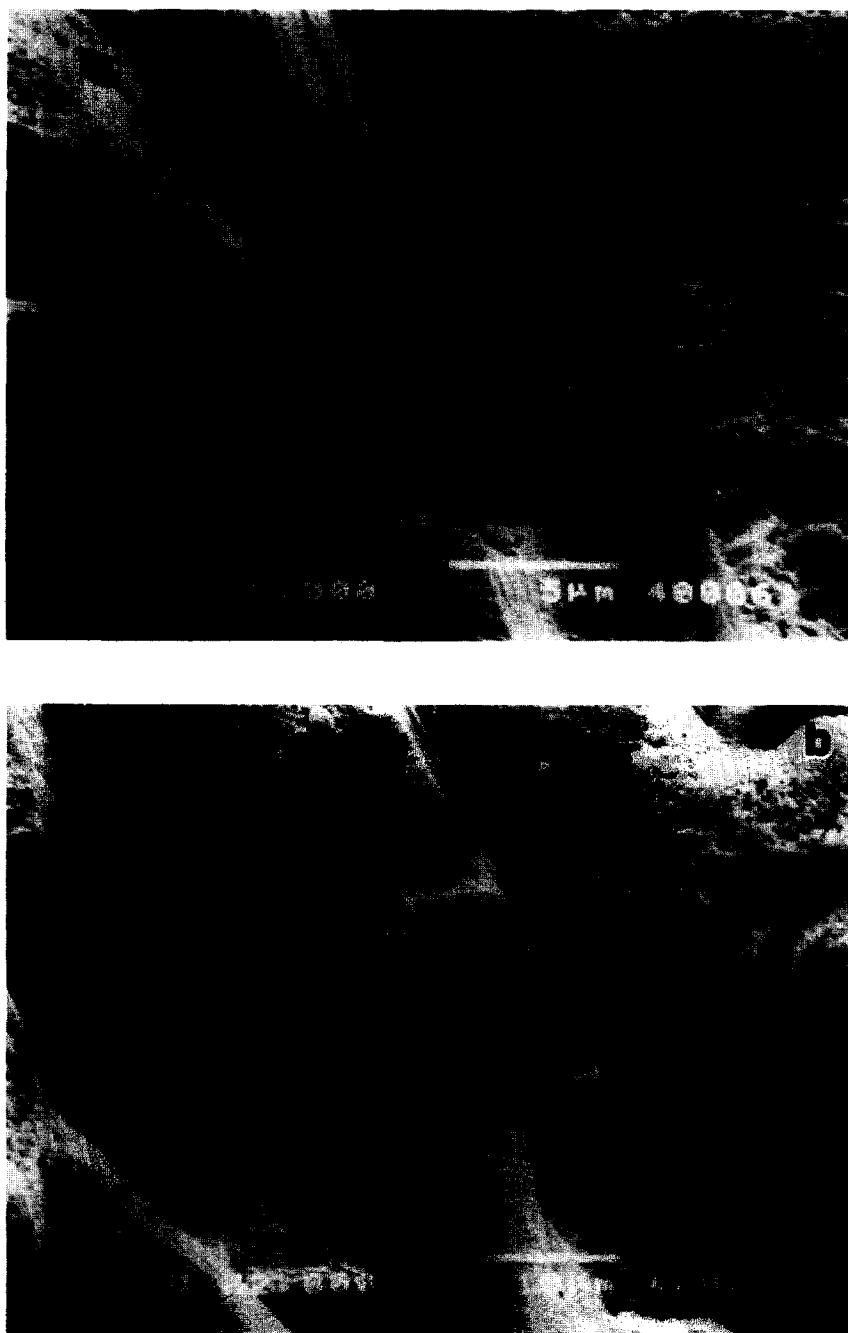


**Fig. 11.** SEM photomicrograph of a composite of  $w/b = 0.40$  and  $SF = 0\%$  aged in hot water for 56 days. (a) Pullout fiber hole, (b) a fiber subjected to bending stress.

line environment of the cement matrix. It can be seen that the fiber surface is uniform without any defect, indicating that the fiber did not suffer from any chemical deterioration, as happens for glass fiber.<sup>6</sup> Therefore, the loss of strength and toughness with age can not be related to any deterioration of the fiber.

### 3.3.2 Pore structure

Pore size distribution and the total porosity of all pores larger than 3 nm were determined by

mercury intrusion porosimetry as described earlier. Figure 13 presents typical pore size distribution of a composite of  $w/b = 0.40$  and silica-fume content of 0 and 28% at ages of 1 day and H230 days. The pore size distribution curves of other composites having silica-fume contents between 0 and 28% were in between the curves in Fig. 13, for each of the respective ages.

It can be seen from Fig. 13 that at the age of one day the silica-fume affects mainly the threshold diameter, and the influence on the total poros-





Fig. 12. SEM photomicrograph of a fiber surface in a composite of  $w/b = 0.25$  and  $SF = 28\%$ , aged in hot water for 56 days.

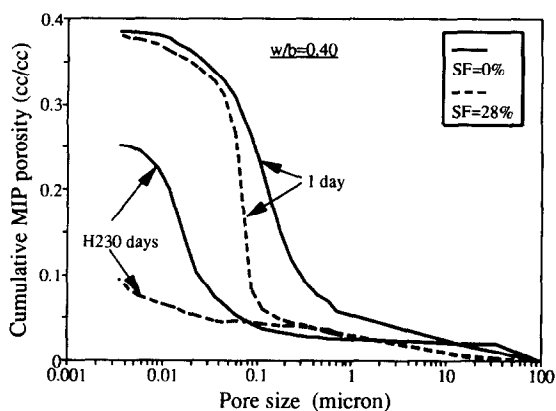


Fig. 13. Pore structure of a composite of  $w/b = 0.40$  and silica fume content of 0 and 28% at the ages of 1 day and H230 days.

ity is very small. With the advance of the hydration process up to the age of H230 days, the effect of the silica-fume becomes more significant: the pore size distribution is changed and the total porosity is reduced markedly. While a clear threshold was observed at the composites without silica-fume, no clear threshold could be seen for composites with silica-fume, indicating a continuous distribution of pore sizes.

The effect of age on the total porosity is presented in Figs 14(a) and 14(b) for aging at 20 and 60°C, respectively. Values for two silica fume contents of 0 and 28% were plotted in the figures for each  $w/b$  ratio. Porosity values for other silica-fume contents, between 0 and 28%, fall in between the corresponding lines at each  $w/b$  ratio.

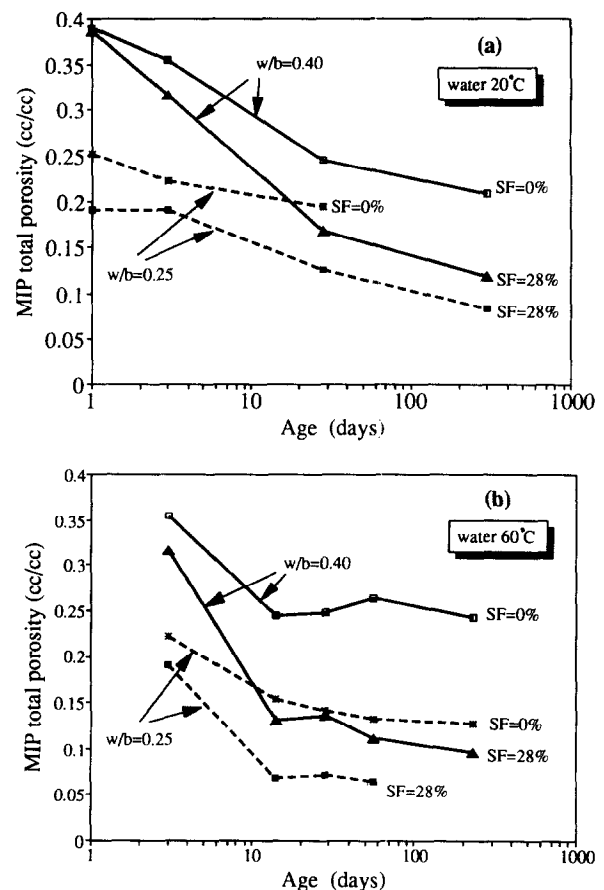


Fig. 14. Effects of age on the total porosity of the composites aged at (a) 20°C and (b) 60°C.

It seems that the rate of change in the total porosity is higher for the specimens aged in hot water. In these specimens, the major change in the total porosity occurred at the ages of 3–14 days, and

after 14 days the rate became more moderate. For the specimens aged at 20°C (Fig. 14(a)) it seems that the total porosity was decreasing continuously with time (with approximately a constant rate along the log time scale). On the basis of the porosity values, it might be concluded that the majority of the hydration process took place during the first two–three weeks for the two aging temperatures (the time scale in Fig. 14 is logarithmic), but the rate was higher for the composites aged in hot water.

#### 4 SUMMARY AND CONCLUSIONS

Long term properties of carbon fiber reinforced cementitious composites were evaluated. Flexural tests showed an increase in strength and toughness of the composites with age up to a maximum at two–four weeks, and a reduction of up to 65% thereafter. Matrix microhardness and flexural strength of the plain matrix showed a continuous increase with age, accompanied by densification of the pore structure.

For a given age, a maximum in flexural strength and toughness was observed at an intermediate silica-fume content of 7–14%. This trend is superimposed on the trend of reduction in properties of the composites after aging for longer periods. SEM observations did not show any chemical attack on the fibers, whereas the matrix became denser, as determined by mercury porosimetry.

These results indicate that CFRC may, under certain conditions, exhibit loss in mechanical properties, which can not be correlated with loss in strength of the matrix or chemical attack on the fibers. In fact, some of the trends suggest that reduction in flexural strength and toughness may occur when the matrix is becoming denser, as observed for high silica-fume contents and after longer periods of aging. These trends suggest that mechanisms other than matrix or fiber deterioration may play an important role in controlling the long term performance of CFRC.<sup>26</sup>

#### REFERENCES

1. Akihama, S., Suenaga, T. & Bannot, T., Mechanical properties of carbon fiber reinforced cement composites and the application to large domes. KICT Report No. 53, 1984.
2. Banthia, N. & Sheng, J., Micro-fiber reinforced cementitious materials. In *Proc. Mater. Research Soc.*, No. 211, Pittsburgh, PA, 1991, pp. 25–32.
3. Ohama, Y., Amano, M. & Endo, M., Properties of carbon fiber reinforced cement with silica-fume. *Concrete International: Design and Construction*, **7** (3) (1985) 58–62.
4. Nishioka, K., Yamakawa, S. & Shirakawa, K., Properties and applications of carbon fiber reinforced cement composites. *Proc. RILEM Symp. 1986: Development in Fiber Reinforced Cement and Concrete*, Paper 2.2, Sheffield.
5. Akihama, S., Suenaga, T. & Banno, T., Mechanical properties of carbon reinforced cement composites. *Int. J. of Cement Composites and Lightweight Concrete*, **8** (1) (1986) 21–33.
6. Bentur, A. & Mindess, S., *Fiber Reinforced Cementitious Composites*. Elsevier Science Ltd, 1990.
7. Laws, V., The efficiency of fibrous reinforcement of brittle matrices. *J. of Phys. D. Appl. Phys.*, **4** (1973) 1737–46.
8. Ali, M. A., Majumdar, A. J. & Ryment, D. L., Carbon fiber reinforcement of cement. *Cement and Concrete Research*, **2** (1972) 201–12.
9. Balaguru, P. N. & Shah, S. P., *Fiber Reinforced Cement Composites*. McGraw Hills Inc., NY, 1992.
10. Katz, A. & Bentur, A., Mechanical properties and pore structure of carbon fiber reinforced cementitious composites. *Cement and Concrete Research*, **24** (2) (1993) 214–20.
11. Soroka, I., *Portland Concrete and Cement Paste*. Chemical Publishing Co. Inc., NY, 1979.
12. Barr, B., Asghari, A. & Hughes, T. G., Tensile strength and toughness of FRC materials. *The Int. J. of Cement Composites and Lightweight Concrete*, **10** (2) (1988) 101–7.
13. Johnston, C. D., Definition and measurement of flexural toughness parameters for fiber reinforced concrete. *Cement, Concrete and Aggregates*, **4** (1982) 53–60.
14. Roßler, M. & Odler, I., Investigation on the relationships between porosity, structure and strength of hydrated Portland cement pastes. 1. Effect of porosity. *Cement and Concrete Research*, **15** (2) (1985) 320–30.
15. Kurbus, B., Bakula, F. & Gobrovssek, R., Reactivity of SiO<sub>2</sub> fume from ferrosilicon production with Ca(OH)<sub>2</sub> under hydrothermal conditions. *Cement and Concrete Research*, **15** (1985) 134–40.
16. Wise, S., Jones, K., Herzfeld, C. & Double, D. D., Chopped steel fiber reinforced chemically bonded ceramics (CBC) composites. In *Materials Research Society Proc. Bonding in Cementitious Composites*, Vol. 114, ed. S. Mindess and S. P. Shah, 1987, pp. 197–203.
17. Soroushian, P. & Bayasi, Z., Silica fume effect on the pullout behavior of randomly oriented steel fiber from concrete. *Proc. Material Research Society, Symp. Bonding in Cementitious Composites*, Vol. 114, eds. S. Mindess and S. P. Shah, 1987, pp. 187–96.
18. Feldman, R. F. & Cheng Yi, H., Properties of Portland cement silica fume pastes. I. Porosity and surface properties. *Cement and Concrete Research*, **15** (1985) 765–74.
19. Larrard, F. & Roy, R. L., The influence of mix composition on mechanical properties of high performance silica fume concrete. *4th Int. Conf. on Fly Ash, Silica Fume, Slag and Natural Pozzolans in Concrete*, Istanbul, May 1992.
20. Larrard, F., Creep and shrinkage of high strength field concrete. *2nd Int. Conf. on Utilization of High Strength Concrete*, ACI SP 121-28, May 1990, pp. 577–98.
21. Paillere, A. M., Buil, M. & Serrano, J. J., Effect of fiber addition on the autogenous shrinkage of silica-fume concrete. *ACI Materials J.*, **86** (2) (1989) 139–44.

22. Bloom, R. & Bentur, A., Restrained shrinkage of high strength concrete. *High Strength Concrete Proc. Int. Conf.*, Lillhammer, Norway, June, 1993, pp. 1007-14.
23. Wei, S., Mandel, J. L. & Said, S., Study of the interface strength in steel fiber reinforced cement based composites. *ACI Materials J.*, **83** (1986) 597-605.
24. Scrivener, K. L., Bentur, A. & Pratt, P. L., Quantitative characterization of the transition zone in high strength concrete. *Advances in Cement Research*, **1** (4) (1988) 230-7.
25. Goldman, A. & Bentur, A., The influence of microfillers on enhancement of concrete strength. *Cement and Concrete Research*, **23** (1993) 962-72.
26. Katz, A. & Bentur, A., Mechanisms and processes leading to changes in time in the properties of CFRC. *Advanced Cement Base Materials J.* (submitted).